Vol. 303: 73–90, 2005 | MARINE ECOLOGY PROGRESS SERIES
Mar Ecol Prog Ser | Published November 21

Development of a stable-isotope constraint system for estuarine food-web models

Peter M. Eldridge[1,*], Luis A. Cifuentes[2], James E. Kaldy[1]

[1]US Environmental Protection Agency, WED/CEB, 2111 SE Marine Science Center Drive, Newport, Oregon 97365, USA
[2]Department of Oceanography, Texas A&M University, College Station, Texas 77843, USA

ABSTRACT: Since the mid-1970s, stable carbon isotopes have been used extensively to address diverse questions related to estuarine carbon cycling. Initially, the isotopic approach was used to identify sources of organic matter and to determine their fate in estuarine food webs. Results obtained with this technique were qualitative; however, more recent attempts to quantify sources or processes have typically relied on simple 2 or at most 3 end-member mixing models. The key assumption is that sources can be defined by a discrete value. This assumption often does not hold and, more importantly, the isotopic variation observed within sources contains significant information. In contrast, inverse-modeling of estuarine carbon cycling has the advantage that ranges of field and laboratory measurements and historical information can be utilized by this method. We used the inverse approach to revisit the issue of a headwater delta's contributions to an estuarine food-web under conditions of low freshwater inflow and after a flood-induced inundation of the delta (Rincon Delta, discharging into Nueces Bay, Texas, USA). We illustrate how isotopic constraints enhance results obtained with more traditional constraint systems. The results suggest that although benthic infauna production is stimulated by increased water flow and delta freshwater inundations, most of the allochthonous carbon is exported from Nueces Bay.

KEY WORDS: Food webs · Stable isotopes · Estuarine processes · Carbon cycling

INTRODUCTION

Anthropogenic activities in rivers and their watersheds have altered the timing, magnitude, and nature of material inputs to estuaries (Hopkinson & Vallino 1995), which in many areas has led to increasing incidence of eutrophication (Nixon et al. 1996). However, there is much uncertainty as to how anthropogenic and other allochthonous inputs affect the biogeochemical functioning and biological community structure of estuarine ecosystems (Cloern 2001). Vollenweider (1975) developed models that show linear relationships between phosphorus loading and chlorophyll in lakes, and similar relationships can be developed in deep-water estuaries (Nixon et al. 2001). These relationships are generally absent from shallow estuarine systems, where submerged aquatic vegetation (SAV), benthic–pelagic coupling and sedimentation distort simple dose–response relationships between nutrients and chlorophyll concentrations (Nixon et al. 2001).

Volterra (1926) proposed a simple, aquatic, food-web model of fish species solved as a system of ordinary differential equations. This model can deal with predator–prey, competition and mutualism or symbiosis, and has evolved into more sophisticated aquatic models such as the nutrient–producer–zooplankton (NPZ) model (Fasham et al. 1990). In the late 1980s and early 1990s a food-web modeling method was developed that provides a unique and consistent system description when there is not enough information available to fully define the system (Vezina & Platt 1988). This modeling technique can encompass a relatively large number of food-web compartments and hence illustrates how allochthonous and autochthonous inputs may be used within an estuarine food web. Food-web analyses are typically solved using mathematical techniques by which independent variables (material flows) are estimated from observation of dependent variables (biomass, for example) and as such are referred to as inverse problems (Vezina et al. 2000).

*Email: eldridge.pete@epa.gov

The inverse modeling approach has been used to describe various aquatic food webs including coral reefs (Niquil et al. 1998), and pelagic ocean and coastal (Vezina & Platt 1988, Jackson & Eldridge 1992), and benthic (Eldridge & Jackson 1993) and estuarine (Vezina et al 2000) systems. While the inverse aquatic food-web model can describe most of the important food-web flows in complex ecosystems, the method requires species-specific information to distinguish differences in material flows among organisms of similar size and life-history (Vezina & Platt 1988, Jackson & Eldridge 1992). Hence when measured fluxes or biomass are not available for these sympatric species, it is necessary to provide some other criteria that can be use to assign the material flow among compartments (e.g. free energy between redox species to differentiate between different anaerobic bacteria: Eldridge & Jackson 1993). For our estuarine food-web model we used stable-isotope data to assign resources among species, given the multiple allochthonous and autochthonous sources available in an estuary.

Carbon-isotope biogeochemistry has been used extensively to describe sources and sinks of organic material in estuaries (see Lajtha & Michener 1994). Thus, incorporation of stable isotope data into inverse food-web analysis should provide simulations that assess feeding strategies of similar species as long as the nutritional sources have distinct isotope ratios.

To develop a mass-balance model such as our inverse model using stable isotopes, we had to also consider the kinetic isotope effects associated with metabolism. For carbon, the isotope effects or fractionation factors ($\varepsilon = \delta^{13}C_{sink} - \delta^{13}C_{source}$) are a consequence of preferential uptake or loss of the lighter, more reactive ^{12}C isotope. The largest of the carbon-isotope fractionations results from photosynthetic carbon fixation due to preferential uptake of ^{12}C from dissolved inorganic carbon (DIC) (–10 to –20‰; Fogel & Cifuentes 1993). Much smaller fractionations occur through heterotrophic assimilation of dissolved organic carbon (DOC) by bacteria (–2 to +2‰; Coffin et al. 1994) and trophic-level transfers between heterotrophs (~ +1‰; Peterson & Fry 1987). Other estimates of the trophic transfer range from 0.4 ± 1.3‰ (Post 2002), and shifts for consumers analyzed as muscle seem to be even higher –1.3 ± 0.3‰ (McCutchan et al. 2003). Similar types of fractionations occur in nitrogen-isotope geochemistry.

We used the inverse analysis with stable-isotope constraints to quantify the marsh and river inputs to Nueces estuary, Texas, and to trace the estuarine food-web response to each of these inputs. The analysis was designed to contrast the differences in the Nueces estuary food-web during a wet summer in which the headwater marsh was inundated repeatedly to a dry summer in which the marsh was rarely inundated. The main differences between these analyses were river input of organic carbon and the isotope ratio of the marsh-derived organic matter.

MATERIALS AND METHODS

Inverse model. Inverse models use a system of linear difference equations to describe the mass-balance and structure of a food web and a system of inequality relationships to specify other associations for which ranges of data represent a parameter better than the mean value. Physiological information and biological field data are temporally and spatially variable and are often best represented as a bounded range of values rather than as a mean value (Vezina et al. 2000). Similarly, temporal and spatial variability occurs in stable isotope data and can usually be linked to variations in the biology and geochemistry of an ecosystem.

We used a non-linear inversion routine from Matlab® 'fmincon' (available at: www.mathworks.com) to estimate all the food-web flows in this analysis; 'fmincon' uses an initial estimate to find a constrained minimum for all flows in the network. A user-defined objective function was provided to 'fmincon', which minimized the squared flows in the network ($\|Ax - b\|$). The routine had the additional requirement that the solution be consistent with the constraints ($Gx \geq h$) and that all x be ≥ 0. A is a matrix of equations describing the geochemical and food-web interaction; x is a solution vector; b is a vector of zeros and data values (as means) for the mass balance equations; G is a set of inequalities that bound ranges of data used in the model, physiological information, and isotope information; and h specifies the bounds that the inequality must satisfy (Vezina et al. 2000, 2004).

The biological compartments for the Nueces Bay analysis consisted of phytoplankton, macroalgae, bacteria, mesozooplankton, fishes (i.e. fishes and shrimp), and benthic infauna; the chemical compartments comprised dissolved organic carbon (DOC), dissolved inorganic carbon (DIC), bottom sediment and detritus, where 'bottom sediments' aggregates sediment biogeochemical processes into 1 compartment. There were additional flux terms representing exchange with Corpus Christi Bay, Rincon Delta, Nueces River and the atmosphere. All carbon flows were replicated for ^{12}C and ^{13}C. The ^{13}C flows, which are typically 1% of the ^{12}C, were multiplied by 100 to normalize ^{13}C flows to the ^{12}C flows, effectively non-dimensionalizing the problem. This procedure keeps the optimization routine from emphasizing the minimization of the ^{12}C flows at the expense of the smaller ^{13}C flows. At the end of the analysis, ^{13}C flows were converted back to

the original units and a $\delta^{13}C$ value for each flow was calculated from the ^{13}C and ^{12}C flows:

$$\delta^{13}C_{i,j} = \left(\frac{\frac{^{13}\text{flow}_{i,j}}{^{12}\text{flow}_{i,j}}}{\left(\frac{^{13}C}{^{12}C}\right)_{\text{std}}} - 1 \right) \times 10^3 \quad (1)$$

where $\text{flow}_{i,j}$ represents the ^{12}C and ^{13}C flow between a source (i) and a destination (j) compartment and $(^{13}C{:}^{12}C)_{\text{std}}$ is the Pee Dee belemnite standard ratio for carbon stable-isotope natural abundance (Craig 1953).

Isotope constraints. A basic assumption of stable-isotope geochemistry is that an organism assimilates both the ^{12}C and ^{13}C of a resource. The ^{13}C flow to an organism is simply calculated from the ^{12}C flow and the $^{13}C{:}^{12}C$ isotope ratio (r_i) of the source compartment by

$$^{13}\text{flow}_{i,j} = r_i {}^{12}\text{flow}_{i,j} \quad (2)$$

A trophic fractionation occurs as part of assimilative (Hatch et al. 2002) and dissimilative processes (Minagawa & Wada 1984, Peterson & Fry 1987), requiring that an additional fractionation be applied to equations for physiological processes:

$$^{13}\text{flow}_{i,j} = r_i \alpha_{i,j} {}^{12}\text{flow}_{i,j} \quad (3)$$

where $\alpha_{i,j}$ expresses the magnitude of isotopic separation or fractionation between source and destination compartments and is related to ε which defines the isotope fractionation in δ notation:

$$\alpha_{i,j} = \left(\frac{\varepsilon_{i,j}}{1000} + 1 \right) \text{pdb} \quad (4)$$

In this model we applied a trophic fractionation factor to the respiration flow of 1‰ for presumed herbivores or 2‰ for carnivores (Appendix 1). Autotroph isotope geochemistry differs from that of heterotrophs in that the autotrophs can preferentially take up ^{12}C from a mixture of ^{12}C and ^{13}C in DIC. The model treats this fractionation in the same way as the trophic fractionation, but in this case the flow is from DIC to an autotroph (Eq. 3). The equation form of the isotope constraint was used for all physiological flows and for biotic to biotic compartment grazer flows to assure that the isotope ratio of flows exiting biotic compartments were the same (except for the trophic fractionation). For non-living food-web compartments, the uncertainty in the data can be taken into account by rewriting equality (Eqs. 2 & 3) as an inequality:

$$-r_i {}^{12}\text{flow}_{i,j} + {}^{13}\text{flow}_{i,j} \geq 0 \quad (5)$$

The minimum inequality constraint is the lower bound of the isotope data for a given compartment or allochthonous input. Multiplying a minimum inequality by –1 converts it to a maximum inequality. The minimum and maximum isotope values used in the 2 inequalities bound the measured range of isotope values allowed by the model for a single food-web flow from a non-living compartment. Each carbon flow within the food-web can be provided with an isotope equality or set of inequalities. Appendix 1 provides a complete description of equations and constraints used in these models. Isotope constraints can also be developed for natural abundance of nitrogen, oxygen, or sulfur using Eqs. (1) through (5).

Sensitivity of food-web flows to isotope ratios. Sensitivity analysis shows how variations in isotope ratios of autochthonous food-web components affect the food-web flow structure. For this analysis, we removed the isotopic constraints for detritus and DOC from Rincon Delta, essentially allowing the analysis to determine the isotopic character of these flows. In separate simulations for the model compartments, the isotope constraints were incrementally increased from –28 to –14‰. We then developed regressions of the relationship between the weighed average of $\delta^{13}C$ for all food-web flows and the weighted $\delta^{13}C$ of flows through the individual compartments. The weighted average $\delta^{13}C$ for individual compartments or for the total food-web is

$$\delta^{13}C(x) = \frac{\sum_{i=1}^{n} (\delta^{13}C(x)_i \times \text{flow}(x)_i)}{\sum_{i=1}^{n} (\text{flow}(x)_i)} \quad (6)$$

where x is the individual model compartment $\delta^{13}C(x)$ or the integrated set of flows that make up the food web $\delta^{13}C(x = \text{total})$. Similarly n is either the number of flows going through compartment x or the total set of flows in the food web. The regression is then calculated from the weighted individual compartment $\delta^{13}C(x)$ and the $\delta^{13}C(\text{total})$ from the sensitivity model runs. The slope and intercept of each regression are examined in this analysis.

Sensitivity to model parameters. We tested effects of data variability on the analysis by increasing and decreasing the value of each datum individually by 20%. The sensitivity of the model to these changes was determined by calculating 2 measures of food-web response to a parameter change. The first is the ratio of the grazer carbon metabolism to the community metabolism (C_m)

$$C_m = \frac{C_{gr}}{C_T} \quad (7)$$

where C_{gr} and C_T are summed grazer and total community respiration. Because there is no growth in this steady-state analysis, respiration is a good measure of an organism's use of organic resources and, by extension, is a useful measure of the entire community's performance. All other carbon pathways that lead through

compartments are simply transformations of organic material (Eldridge & Jackson 1993). The second sensitivity index is based on root mean-squared difference (RMSD) between output from the standard model and the model results, with 1 parameter changed at a time. We normalize RMSD (N-RMSD) by dividing the RMSD by the average value of the standard model result.

We used a sensitivity index $S(A,p)$ developed by Fasham et al. (1990) to relate a change in an input parameter to a change in the model output (A). A is either C_m or N-RMSD for our 2 sensitivity tests. For each, the change in a variable (A) relative to a change in a parameter p is

$$S(A,p) = \left(\frac{A(p)-A_s}{A_s}\right)\left(\frac{p-p_s}{p_s}\right)^{-1} \times 100 \qquad (8)$$

where p_s and p are the standard and changed parameter values and A_s and $A(p)$ are the standard and changed A. We calculated S as a percentage change in the output for each change made in a model input parameter. If S for a parameter (p) is zero then A does not change with p. If S is 100%, a 20% increase in p caused a 20% increase in A. For $S > 100\%$, A is disproportionately large relative to a change in the input parameter (Eldridge & Jackson 1993, Fasham et al. 1990).

Network analysis. Ulanowicz & Kay (1986) assembled several techniques for analyzing food webs into the software package NETWRK4.2a that we applied to the results of our inverse analysis. Although NETWRK software provides a number of measures of ecological function within a food web, we confine our use to dependency coefficients and input–output analysis. The dependency coefficient describes the extent to which each component of the food web depends on every other component of the food web; i.e. the fraction of the total amount entering a food-web component that ultimately came from each possible resource. The input–output analysis provides a decomposition of each input so that we can isolate the effect of both allochthonous and autochthonous inputs to each estuarine food-web compartment and to export from the estuary.

Study sites. Nueces Bay is a secondary bay located to the north of Corpus Christi, Texas. Nueces River and Rincon Delta discharge into the western end of Nueces Bay while Corpus Christi Bay exchanges water with the mouth of the Nueces Bay (Fig. 1). On average, Nueces Bay receives 7.8×10^5 m^3 yr^{-1} of freshwater from Nueces River and Rincon Delta and has a hydraulic residence time of 0.46 yr, resulting in an average salinity of 21 (Longley 1994). Rincon Delta is roughly the same size as Nueces Bay and is vegetated with high marsh plants typical of mesohaline marshes in coastal Texas (Longley 1994). Freshwater inflow to Nueces Bay comes primarily from the

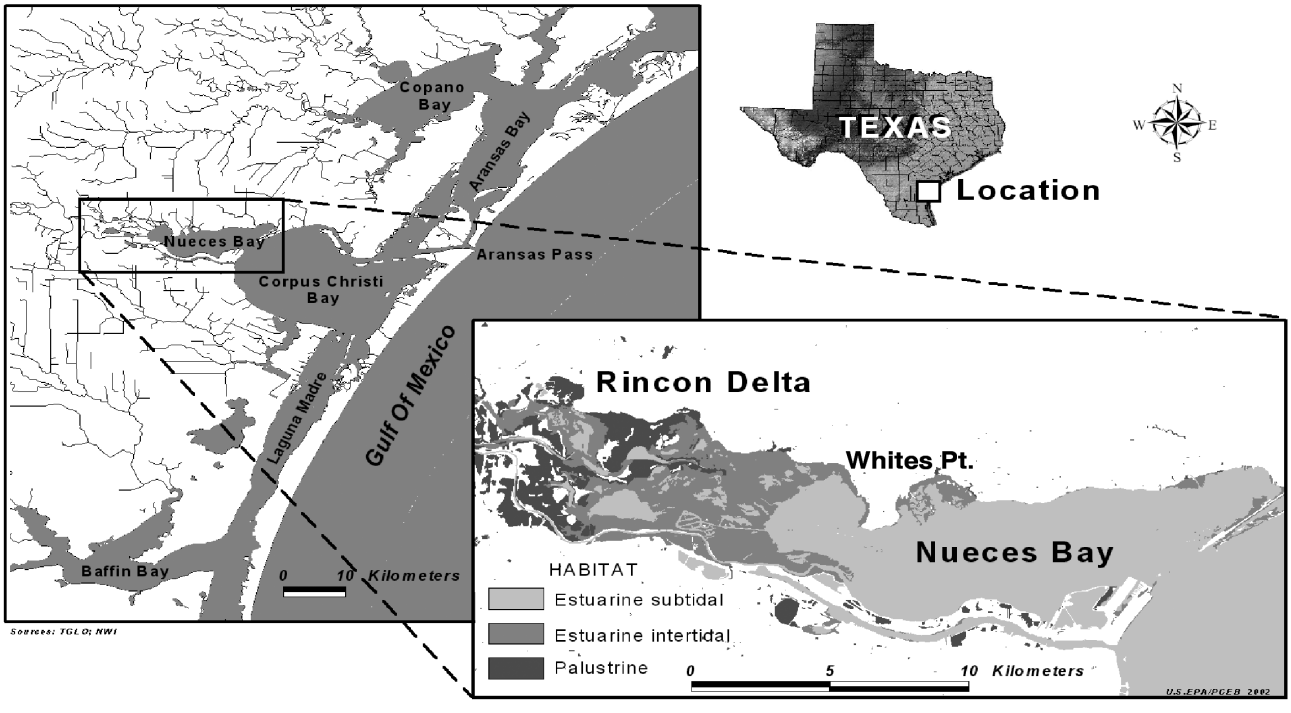

Fig. 1. Nueces Bay and Rincon Delta, Texas. Nueces Bay is a secondary estuary with a headwater delta (Rincon Delta) roughly of the same size as the bay. The delta is composed of extensive intertidal marsh and palustrine habitat

Nueces River. Above the head of the Rincon Delta, the Bureau of Reclamation (2000) created a shallow sill that under high-flow and river-stage conditions shunts a portion of the river flow through Rincon Delta, otherwise most of the freshwater inflow to Nueces Bay enters through the river. Gauged freshwater inflow rates through Nueces River (US Geological Survey 08211500) and Rincon Delta (US Geological Survey 08211503) allowed us to calculate loading rates to Nueces Bay.

Nueces Bay is shallow (<1.8 m) and well-mixed by wind-generated waves and generally considered a negative estuary (Twilley et al. 1999). In a negative estuary evaporation exceeds the freshwater supply from rivers and from local rain, and as a consequence the water in the estuary is more saline than in the open ocean (see: www.ozestuaries.org/oracle/ozestuaries/conceptual_mods/cm_glossary.htm). The Bay is microtidal, with a tidal range between 0.2 and 0.8 m (see: www.co-ops.nos.noaa.gov).

Field collection methods and data acquisition. There is a large database available for ecosystem modeling of Nueces Bay including organism production and growth rates (see Table 1), and a fairly complete set of published stable isotope data for the bay (see Table 2) and for Rincon Delta plants (see Table 3).

In addition to historical data, we recorded DIC and DOC concentrations and stable-isotope ratios (see Fig. 2) and photosynthetic pigments during the summer of 1998. Our measurements also included nutrients (nitrate, nitrite, ammonium, urea, orthophosphate, and silicate) temperature and salinity. Texas Water Development Board (TWDB) (see: http://hyper20.twdb.state.tx.us/data/bays_estuaries/b_nEpage.html) and the Texas A&M-Corpus Christi University, Division of Nearshore Research (see: http://lighthouse.tamucc.edu/pquery) made continuous measurements of temperature, salinity and water flow at several stations in Nueces River and its estuary.

Water samples for our survey were collected from the surface at 16 stations between the Nueces River and the outlet to Corpus Christi Bay over a 12 h period, providing a nearly synoptic data set. We used a stratified random sampling design for the study. At each station, 20 l water samples were pumped into a cubitainer from 0.5 m depth with a peristaltic pump. Samples for analyses were then drawn from the cubitainer and filtered. All subsampling was conducted in the field. Triplicate subsamples for DIC (30 ml) were transferred to clean Quorpak bottles, fixed with mercuric chloride, sealed and placed on ice. Triplicate subsamples for DOC (5 to 10 ml) were filtered through precombusted GFF filters into acid-washed and combusted scintillation vials, and frozen immediately on dry ice. For pigment samples, 1 l of water was filtered through GF/F filters, placed in labeled Petri dishes and stored in liquid nitrogen. For nutrient analysis we used 30 ml of filtrate from the pigment-analysis samples. Samples were returned to Texas A&M University and analyzed for concentration and $\delta^{13}C$, DOC, DIC (Salata et al. 1996), nutrients (Parsons et al. 1983), and pigments (Mantoura & Llewellyn 1983). These data were then used in the inverse analysis of carbon flow in the Nueces estuary.

Data treatment. Flux and biomass data with units of m^{-3} were converted to m^{-2} by multiplying by the average water depth (1.8 m). Macroalgae biomass (*Gracilaria* sp.) was concentrated between Whites Point and Rincon Delta with lower concentrations throughout the bay. Because of the uncertainty in this data we used the same broad biomass constraint (0.64 to 58 mg dry wt m^{-2}) as used in the Laguna Madre analysis (Kaldy et al. 2002) so that the model would estimate the macroalgal fluxes. *Gracilaria tikvahiae* has between 28 and 37% carbon per unit of dry weight (Penniman & Mathieson 1987). We assumed for this analysis that 33% of the dry weight was carbon.

Mesozooplankton production as *Acartia tonsa* averaged 9.0 with a range from 0.6 to 56 mg C m^{-3} d^{-1} during summer. We assumed that *A. tonsa* production was 70% of the total zooplankton production (Longley 1994 estimates 70 to 85% of macrozooplankton is *A. tonsa* and barnacle larvae.)

Burial rate was taken from Brock 2001 assuming a sediment C:N of 10 to 20 (this study).

Mesozooplankton biomass was taken as the geometric mean of day-time samples. Microzooplankton and macrozooplankton have about the same biomass in Nueces estuary (Longley 1994). Given that the microzooplankton range from 24.6 to 207.2 mg dry wt m^{-3} (Longley 1994), we estimated total zooplankton to have a biomass from 50 to 414 mg dry wt m^{-3}. Copepod dry wt is between 35 and 50 % carbon (Parsons et al. 1984). We assumed for this analysis that 40% of the dry weight is carbon.

Infauna biomass was estimated from filter-feeding and deposit-feeding infaunal biomass using Fig. 2.11C in Montagna & Li (1996), assuming that 40% of the macrofauna dry weight was carbon (see Montagna & Kalke 1992).

RESULTS

1998 survey results

Salinity, temperature and dissolved O_2 concentration were relatively constant spatially over the length of Nueces Bay based on our data and temporally (based on TWDB data: data not shown). The O_2 concentrations

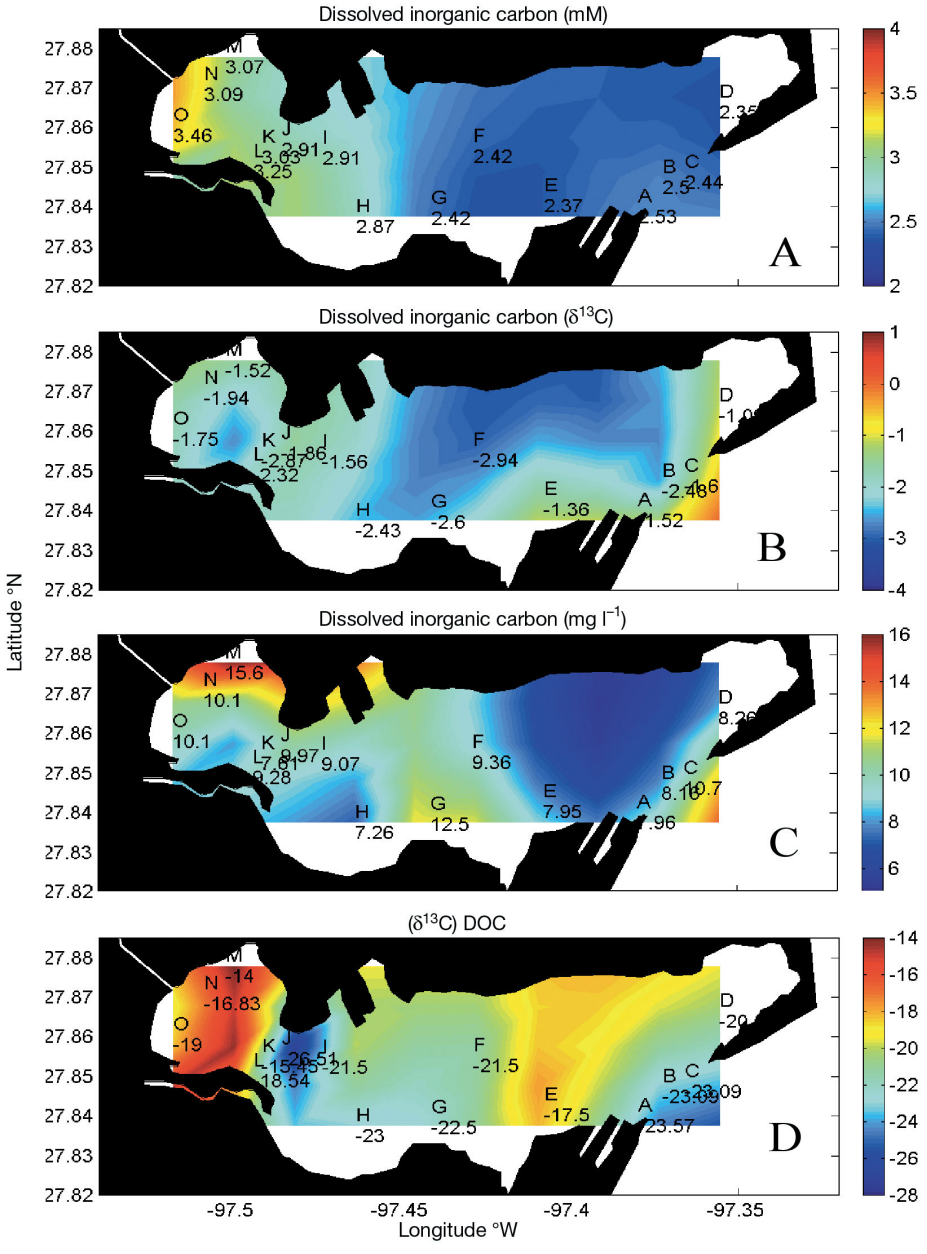

Fig. 2. Carbon concentration and stable-isotope measurements during summer 1998. (A) Dissolved inorganic carbon concentration, DIC; (B) δ^{13}DIC; (C) dissolved organic carbon concentration, DOC; (D) δ^{13}DOC during Nueces survey. A to O: station identifiers

ranged between 8 and 9 mg O_2 l^{-1}. Thus hypoxia was not present at our sampling sites during the survey. DIC and DOC were higher in concentration and generally isotopically heavier at the western end of the estuary, particularly near Rincon Delta (Fig. 2), where C4 plant material contributes up to 70% of the marsh plant biomass (Longley 1994). Flows from the Nueces River were small as the result of low precipitation and reservoir storage during a 1998 drought.

Nutrient concentrations were low during our samplings. Important DIN species were NO_3^- (0.1 and 2.3 µM), NH_4^+ (0.2 to 1.0 µM), and urea (1.0 to 3.5 µM). Orthophosphate ranged from 0.2 to 0.5 µM. Only NH_4^+ and urea showed any spatial patterns, with NH_4^+ most abundant in the NE Nueces Bay, and urea most abundant in the confluence of the Nueces River (data not shown). Chlorophyll levels ranged between 6 and 25 µg l^{-1} in the Bay which is in the medium range in Bricker et al.'s (2003) classification of estuaries. While 19 pigments were measured by the HPLC method, chlorophyll and fucoxanthin were the only abundant pigments in the bay. The relatively high fucoxanthin concentrations (3 to 9 µg l^{-1}) indicate the presence of diatoms in Nueces Bay (Bianchi et al 1997, Roelke et al 1999), which potentially are a good food resource for zooplankton and epi- and infaunal benthic organisms (Roelke et al. 1999). Consequently, the food-web analysis assumed that all consumers had access to phytoplankton. There were also macroalgae mats (*Gracillaria* sp. $\delta^{13}C$ = –18.6 to –21.6‰) in the eastern portion of the bay that were up to 0.5 m thick. The N:P of dissolved inorganic nutrients was substantially lower than the Redfield ratio (16:1), suggesting that the system may have been nitrogen-limited during the summer of 1998.

Models

The objective of our study was to examine differences in food-web structure due to variations in the isotopic character of allochthonous and autochthonous components of the Nueces Estuary food web. In the first sensitivity analysis we altered the DOC and detrital inputs from Nueces River and Rincon Delta to simulate the effects of increased water flow from Nueces River and inundation to Rincon Delta. For these 'flood'

Table 1. Flux and biomass data used in inverse model

	Abbrev.	Range (mmol C m^{-2} d^{-1})	Source
Flux parameters			
Phytoplankton primary production	NPP_{phy}	40–146	Stockwell (1989)
Macroalgae primary production	NPP_{mal}	25–56	Kaldy et al. (2002)
Bacterial production estimate	P_{bac}	5.1	Benner & Yoon (1989)
Mesozooplankton production	GP_{mes}	1.35–8.4	Buskey 1989, Longley (1994)
Infauna production	GP_{inf}	2.1–3.2	Montagna & Li (1996)
Burial	$Fbur_{est}$	4.1–9.8	Brock 2001, this study
River sediment input	$Fsed_{riv}$	1.1–5.8 (low inflows) 21–107 (high inflows)	Longley (1994)
River DOC input	$FDOC_{riv}$	≥ 0.11 (low inflows) ≥ 3.11 (high inflows)	Longley (1994)
Delta export	FOC_{del}	37–116	Longley (1994)
Biomass parameters			
Mesozooplankton biomass	B_{mes}	13.9	Longley (1994)
Infauna biomass	B_{inf}	731	Montagna & Kalke (1992), Montagna & Li (1996)
Fish biomass	B_{fis}	4.5	Longley (1994)

and 'dry' analyses; water flow, detritus and DOC concentration data were available for river and delta inputs to the bay, but the rest of the data were the same for both simulations (Tables 1 & 2). NETWRK analysis was then used to reveal the changing character of the system with perturbed inputs to the food web. In the second sensitivity analysis we developed regressions between flow-weighted isotope ratios of each compartment and an integrated value for the food web to show how individual populations alter the estuarine food web (see Eq. 6). Finally, in a stability analysis we related changes in all model inputs to changes in the model output.

Most of the organic loading to Nueces Bay comes from Nueces River and Rincon Delta. Nueces water shed is a semi-arid environment, characterized by prolonged periods of low flows during which the sill between the delta and the river directs most of the freshwater down Nueces River, effectively isolating Rincon Delta from upland water-sources. Storm-driven or dam releases of freshwater result in over-banking of the sill between Nueces River and Rincon Delta, and inundation of the high delta with freshwater. Because of municipal and industrial water demands and dam construction, there are relatively few hydrographic events capable of inundating the Rincon Delta high-marshes. Between 1994 and the end of 1999, only 20 hydrographic events resulted in significant inundations of Rincon Delta (Ward et al. 2002). The isolation of Rincon Delta from freshwater results in increasingly hypersaline soils with increasing distance from Nueces Bay (Alexander & Dunton 2002). These hypersaline soils are a common substrate for cyanobacteria mat development (W. M. Pulich pers. comm.) and consequently cyanobacteria cover much of the open areas (<10 cm above mean low slack-tide)

Table 2. Stable-isotope data used in inverse analysis

Parameter	$\delta^{13}C$	Source
Atmosphere	–8.0	Wahlen (1994)
River DIC	–2.0	This study
Coastal DIC	–1.9	This study
Delta POC and DOC	–13.9 ± 2 low flows –25.0 ± 2 high flows	Parker et al. (1989), Longley (1994), Pulich & Scalan 1987, this study
River POC and DOC	–25 ±3	Longley (1994), Roelke 1997)
Estuarine DOC	–20.0 ± 3.5	This study
Estuarine bacteria	–20.0 ± 3.5	L. A. Cifuentes (pers. data)
Phytoplankton	–21.9 ± 1	Parker et al. (1989)
Macroalgae	–16.7 ± 1.6	Parker et al. (1989)
Mesozooplankton	–18.3 ± 1.5	Longley (1994)
Benthic infauna	–20.5 ± 1.3	Parker et al. (1989)
Fishes	–18.8 ± 1.8[a]	Parker et al. (1989)
Detritus	–21.0 ± 1.7	Parker et al. (1989)
Sediment TOC	–19 ± 1.5	Parker et al. (1989)

[a]Average (±SD) for pelagic and omnivorous benthic fishes, shrimps, decapods, benthic predatory fishes and herbivorous fishes

Table 3. Isotope ratios of upper-marsh (not inundated by 15 cm tides) and lower-marsh (inundated by 15 cm tides) plant species

Species	Carbon fixation	Elevation	$\delta^{13}C$	Source
Salicornia virginica	C3	High + low	–25.7	Pulich & Scalan (1987), Weilhoefer (1998) Dunton et al. (2001)
Borrichia frutescens	C3	High	–26.0	Pulich & Scalan (1987), Weilhoefer (1998) Dunton et al. (2001)
Limnoium nashii	C3	High	–27.1	Weilhoefer (1998), Dunton et al. (2001)
Batis maritima	C3	High + low	–22	Pulich & Scalan (1997)
Lycium caralinianum	no data	High	no data	Dunton et al. (2001)
Suaeda linearis	no data	High	no data	Weilhoefer (1998), Dunton et al. (2001)
Mudflat cyanobacteria	no data	Low	–11.5	Pulich & Scalan (1987), Weilhoefer (1998), Dunton et al. (2001)
Distichilus spicata	C4	High + low	–14.4[a]	Dunton et al. (2001)
Spartina alternifora	C4	Low	–11.6 to –17.4	Benner et al. (1991), Weilhoefer (1998), Dunton et al. (2001)
Monanthochloe litteralis	C4	Low	–15.3	Pulich & Scalan (1987), Weilhoefer (1998), Dunton et al. (2001)

[a]Isotope ratio from North American west-coast marsh (P. M. Eldridge unpubl. data)

that reticulate the low marsh (Dunton et al. 2001). Cyanobacteria mats are isotopically enriched compared to C3 and most C4 plants (Pulich & Scalan 1997, Parker et al. 1989), and may be an important source of dissolved organic material (DOM) and detrital carbon to Nueces Bay. Similarly C4 plants are isotopically enriched compared to C3 plants as a result of the Hatch-Slack carbon fixation pathway. Overall, 70% of the plant materials in Rincon Delta are isotopically heavy C4 plants (Longley 1994), most of which are found in the lower elevations of the delta (Table 3). Portions of the channel margins are dominated by the C4 plants *Distichlis spicata* and *Spartina alterniflora* and the C3 plant *Salicornia virginica* (Dunton et al. 2001). Given the prevalence of C4 plants and cyanobacteria mats in bare areas of the low marsh of the Rincon Delta (Wielhoefer 1998, Dunton et al. 2001), it is not surprising that isotopically heavy DOC (–16 to –12‰) was measured at the boundary of Nueces Bay and Rincon Delta in our survey of Nueces Bay after a prolonged dry period (Fig. 2D). In the inverse model simulation of this time period we therefore used an isotopically heavy boundary condition for Rincon Delta carbon (i.e. –16 to –12‰ for detritus and DOC) (Table 2).

The high-marsh areas of the Rincon Delta are dominated by the C3 plants *Salicornia virginica*, *Borrichia frutescens*, and *Batis maritima* (Weilhoefer 1998, Alexander & Dunton 2002). A high frequency of marsh inundations causes short-term vegetative expansions of the C3 plants *Borrichia frutescens* and *Batis maritima* (Alexander & Dunton 2002). A progression of growth and then loss during a 23 d inundation of Rincon Delta in July 1997 caused the delta tidal channels to be filled with *Borrichia frutescens* and *Batis maritima* detritus (P. M. Eldridge pers. obs.). In an inverse model simulation of this time period we therefore assumed a boundary condition with isotopically light (–23 to –27‰) material composed mostly of detritus and DOC (Table 2).

Low frequency of marsh inundation: 'dry' simulation. The dominant flows of carbon in our 1998, dry summer, food-web analysis 'dry model' followed a path from the autotrophs (phytoplankton and macroalgae) to detritus, mesozooplankton and infauna in about equal proportions. Most of the detritus was either metabolized in the sediment or exported from the bay. Other than bacterial metabolism of sediment, relatively little of the detritus was consumed by the organisms in Nueces Bay. Nearly 60% of the flow into the DOC compartment derived from Rincon Delta and Nueces River, with the rest coming equally from the estuarine autotrophs, mesozooplankton and infauna. Bacteria consumed only a small portion of the DOC with secondary bacterial production being less than 25% of primary production and about two-thirds of mesozooplankton or infaunal consumption (Table 4A).

Phytoplankton and macroalgae provided 62 and 38% of the 72 mmol C m^{-2} d^{-1} of total gross primary production, respectively. Physiological losses from autotrophs were 3.6 mmol C m^{-2} d^{-1} released as CO_2, and an equal amount as DOC. These losses were the minimum allowed by the constraints. Of the remaining 64.8 mmol C m^{-2} d^{-1} net primary production, 24% went to detritus and 76% went to heterotrophs. NETWRK showed that the relative amount of phytoplankton and macroalgae production consumed by heterotrophs was the same (62 versus 67%). However, since macroalgae production was only two-thirds of the phytoplankton production, the dependency on macroalgae was about two-thirds that on phytoplankton (Fig. 3). Infauna was primarily dependent on phytoplankton production while mesozooplankton and fishes were more dependent on macroalgae (Fig. 3A,B).

Community respiration was 70.9 mmol C m^{-2} d^{-1}, suggesting that metabolism and primary production were about the same in the bay (autotroph production to heterotrophic respiration ratio = 1.0). Of the 80.2 mmol C d^{-1} consumed, the infauna used 34%,

Table 4. Exchange matrices for (A) low-marsh and (B) high-marsh inundation-frequency simulations. Row entries: source of flow; column entries: flow recipient. Upper entry in each cell is flow (mmol m^{-2} d^{-1}), lower entry is isotope ratio of flow. phy: phytoplankton; mal: benthic and macroalgae; bac: pelagic bacteria; mes: mesozooplankton; inf: benthic infauna; fis: fishes; dic: dissolved inorganic carbon (CO_2 system); doc: dissolved organic carbon; det: detritus; sed: sediment; riv: riverine carbon loading; del: Rincon delta carbon sources; atm: atmosphere; bur: burial. NaN: $\delta^{13}C$ is not calculated for flows < 0.05

(A)	phy	mal	bac	mes	inf	fis	dic	doc	det	sed	bur	exp
phy				9.5 –21.9	16.9 –21.9	0.0 NaN	2.2 –21.8	2.2 –21.8	13.6 –21.9			
mal				14.6 –16.9	4.9 –16.9	3.8 –16.9	1.4 –17.0	1.4 –17.0	1.7 –17.1			
bac				0.0 NaN	1.7 –19.8		15.7 –20.3	0.0 NaN	0.0 NaN			
mes						0.0 NaN	17.2 –19.3	5.7 –18.2	5.8 –18.3			
inf						5.1 –20.5	12.7 –21.5	4.2 –20.4		5.0 –20.5		
fis							5.8 –20.8	1.9 –19.2	0.0 NaN			2.2 –19.0
dic	44.4 –21.9	27.8 –16.8										2.2 –2.2
doc	0.0 NaN		17.4 –20.2									28.7 –16.7
det				4.6 –19.3	3.4 –22.6	0.0 NaN		0.0 NaN		15.1 –19.3		16.9 –19.3
sed							15.9 –19.0				4.2 –21.9	
riv						1.1 –28.7		6.9 –29.1	5.8 –29.0			
del						0.0 NaN		23.4 –14.0	13.2 –14.0			
atm							3.5 –8.0					
exp							0.0 NaN					

(B)	phy	mal	bac	mes	inf	fis	dic	doc	det	sed	bur	exp
phy				4.7 –22.0	18.9 –21.9	2.3 –21.9	2.2 –21.8	2.2 –21.8	14.1 –21.9			
mal				7.6 –16.8	5.3 –16.7	1.6 –16.8	1.4 –17.0	1.4 –17.0	10.5 –16.9			
bac				0.0 NaN	1.6 –20.3		16.7 –20.2	0.0 NaN	0.2 NaN			
mes						0.0 NaN	5.6 –19.2	1.9 –18.5	4.8 –18.3			
inf						3.8 –20.4	20.7 –21.5	6.8 –20.5		0.8 –20.7		
fis							5.2 –20.8	1.7 –19.0	0.0 NaN			0.8 –18.3
dic	44.4 –21.9	27.8 –16.8										1.1 –2.3
doc	0.0 NaN		18.5 –20.2									26.0 –23.7
det				0.0 NaN	6.3 –22.7	0.0 NaN		5.1 –22.8		23.8 –22.7		30.1 –22.7
sed							18.1 –19.0				6.4 –32.8	
riv						0.0 NaN		3.1 –27.1	21.0 –27.0			
del						0.0 NaN		22.4 –23.0	14.6 –23.1			
atm							3.4 –8.2					
exp							0.0 NaN					

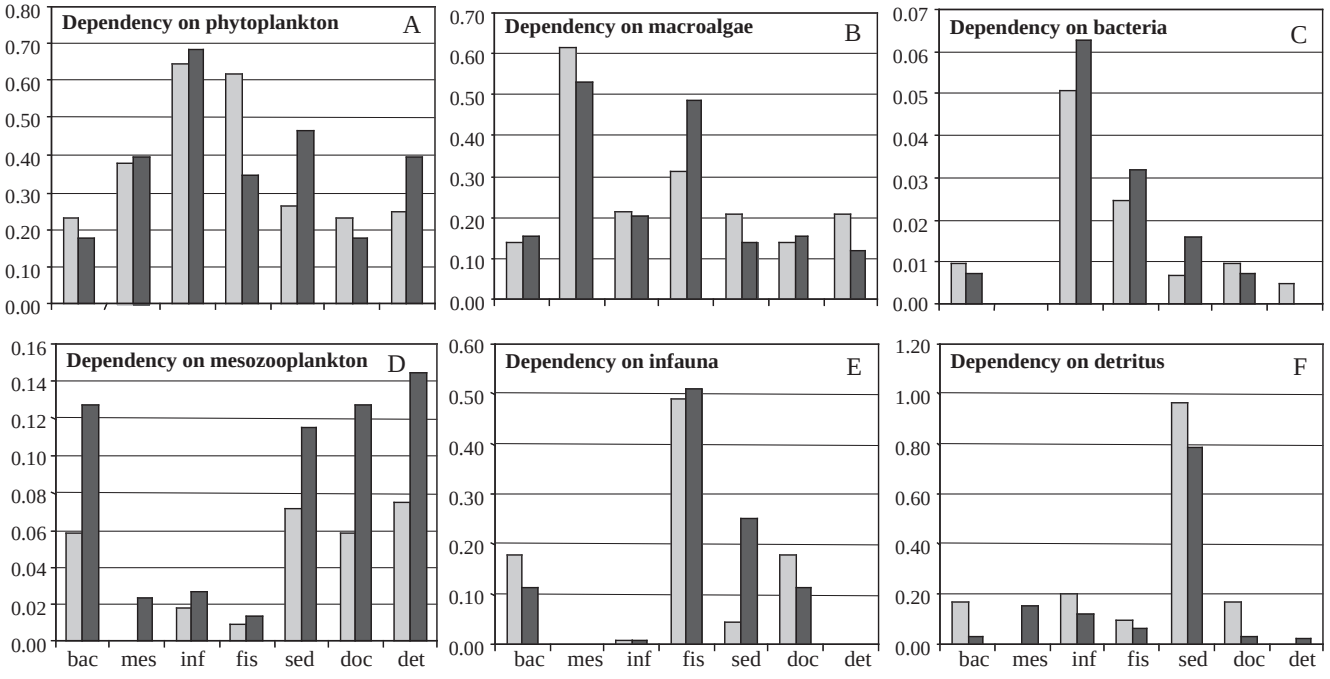

Fig. 3. Dependency of food-web compartments on production of other compartments (bac: bacteria; det: detritus; doc: dissolved organic carbon; fis: fishes; inf: infauna; mes: mesozooplankton; sed: sediment organic carbon). Light-gray columns: flood model; dark-gray columns: dry model. Ordinate quantifies the dependency on a scale of 0 to 1

mesozooplankton 24%, fishes 11%, and bacteria the rest. Bacteria and detritus were not consumed by the fish and comprised about 17% of the mesozooplankton and infaunal consumption (Table 4A).

The total carbon flow through the detritus was 40.1 mmol C m^{-2} d^{-1}, of which 33% came from the delta, 14% from the river, and 14% from mesozooplankton, the rest coming from phytoplankton and macroalgae. Most of the detrital carbon went either to bottom sediments (38%) or was exported (42%) from the estuary, with the balance being consumed by mesozooplankton and infauna.

The total carbon flow through the DOC was 46 mmol C m^{-2} d^{-1} of which 52% came from Rincon Delta, 15% from the river, 8% from autotrophs, and 25% from heterotrophs. Of the carbon leaving the DOC compartment, 62% was exported from the bay and heterotrophic bacteria consumed the rest. Bacteria were wholly dependent on DOC, and ultimately derived additional carbon resources from phytoplankton (17%), macroalgae (13%), mesozooplankton (13%), infauna (11%) and detritus (3%) (Fig. 3A,B,D,E,F).

Allochthonous organic carbon inputs to the estuary were 50 mmol C m^{-2} d^{-1}, of which 26% came from the river and 74% from Rincon Delta. DOC formed 47 and 14% of the organic carbon from the delta and river, respectively, with the remained being detritus.

High frequency of marsh-inundation: 'Flood'. 'Flood' and 'dry' simulations had quantitatively similar patterns of carbon flow within the food web (Table 4B). By far, the major allochthonous carbon flow into the estuary for both the 'flood' and the 'dry' models was through Rincon Delta. Flood and dry simulations had the same autotrophic production, similar mesozooplankton consumption, but the 'flood' model had about 34% greater consumption of infauna by fish organisms. NETWRK analysis also predicted that fish production was more dependent on phytoplankton in the 'flood' model simulation and more dependent on macroalgae in the 'dry' model simulation (Fig. 3A,B). NETWRK further showed that phytoplankton was the major resource for the infauna and there was a strong linkage between infauna and fishes in both the flood and dry simulations.

Comparison of food-web analysis with and without stable-isotope constraints. Here we compare the results of the model with and without isotope constraints. The objective of this analysis was to determine how the isotope constraints affected the model output. We found that of the 52 flows in the food-web analysis, 35 were altered in the presence of the isotope constraints, and that of these 22 flows were altered by more than 20%. The isotope constraints had no effect on autotrophic production, respiration and excretion. The physiological flows (respiration, excretion, fecal) of the heterotrophs generally increased in magnitude when there were isotope constraints. About an equal number of grazer and export flows increased and

Table 5. Exchange matrix showing percentage difference between high and low inundation-frequency simulations (Table 4) with and without isotope constraints. Upper entry in each cell is high-water, lower entry is low-water inundation analysis. NaN: flows calculated with and without isotope constraints were zero. Other abbreviations as in Table 4

	phy	mal	bac	mes	inf	fis	dic	doc	det	sed	bur	exp
phy				−176.0 −30.6	15.4 12.6	−47.6 (3.8)[a]	0.0 0.0	0.0 0.0	45.7 33.5			
mal				−19.7 40.9	−129.1 −125.1	(1.6)[b] (3.8)[b]	0.0 0.0	0.0 0.0	64.1 −217.2			
bac				NaN NaN	13.8 25.1		24.0 25.7	NaN NaN	(0.2)‡ NaN			
mes						NaN NaN	−192.3 15.0	−205.8 15.0	0.5 15.0			
inf						−154.5 −52.3	22.7 −12.2	22.7 −12.3		−800.9 −25.1		
fis							15.3 13.7	15.3 13.7	NaN NaN			−909.9 −118.5
dic	0.0 0.0	0.0 0.0										(1.1)[b] (2.2)[b]
doc	NaN NaN		24.0 25.7									4.5 31.1
det				(3.4)[a] 26.6	−31.2 −71.0	NaN NaN		82.7 NaN		36.6 20.6		14.6 −8.7
sed							25.7 25.2				−30.9 −51.5	
riv						NaN (1.1)[b]		NaN 98.4	0.0 81.0			
del						NaN NaN		15.4 25.3	−23.6 −45.8			
atm							17.0 −59.1					
exp							(2.8)[a] (5.6)[a]					

[a]Zeros for isotopically constrained and value of unconstrained flow in parentheses (units = mmol m^{-2} d^{-1})
[b]Value for isotopically constrained flow in parentheses (units = mmol m^{-2} d^{-1}) and unconstrained flow is zero

decreased with isotope constraints added to the model. Fish migration from the river in the low inundation analysis went to zero without the isotope constraints (Table 5).

Sensitivity analysis

There are 2 aspects of the food-web model addressed in these sensitivity tests: the effect changes in the isotope ratio of autochthonous compartments have on the isotopic character of the food web, and the effect that each model input has on model performance.

Sensitivity to isotope ratio of internal food-web flows. To show how individual components affect the food web, the weighted $\delta^{13}C(x)$ of individual compartments (e.g. DOC, detritus, infauna, etc.) was regressed with the weighted $\delta^{13}C$(total) in successive runs of the model (Eq. 6). The slope of these regressions provides an estimate of how well a food-web component tracks the isotope ratio of all the flows in the food web. For example, if the regression has a slope of 1.0, a sampling of that food-web component would mirror (given no model or sampling error) the weighted isotope ratio of the whole food web. The slopes of the weighted regression for these compartments ranged from 0.09 to 0.24 and fell into 3 discrete groups, with a maximum effect in Group 1 (detritus), with progressively smaller effects for Group 2 (DOC, bacteria, and infauna) and Group 3 (mesozooplankton and fishes) (Fig. 4). Thus none of the food-web components could be used to directly characterize the food web without resorting to the regression. Not surprisingly, the carbon processing rates (throughputs from NETWRK) were in the same descending order of activity as the slopes of these regressions. Hence, the model confirms a rather obvious facet of stable-isotope geochemistry, i.e. the more an organism participates in a food web the more it takes on the isotopic character of that food web.

Food-web sensitivity to changes in parameters. The grazer respiration-sensitivity parameter $S(Cm,p)$ concerns only the food web's biological response to autochthonous and allochthonous inputs (Jackson & Eldridge 1992), whereas the generalized fit parameter $S(N\text{-}RMSD,p)$ is an integration of all the food-web flows and hence shows a smaller response to single parameter changes than the $S(Cm,p)$ (Table 6). Changes in the iso-

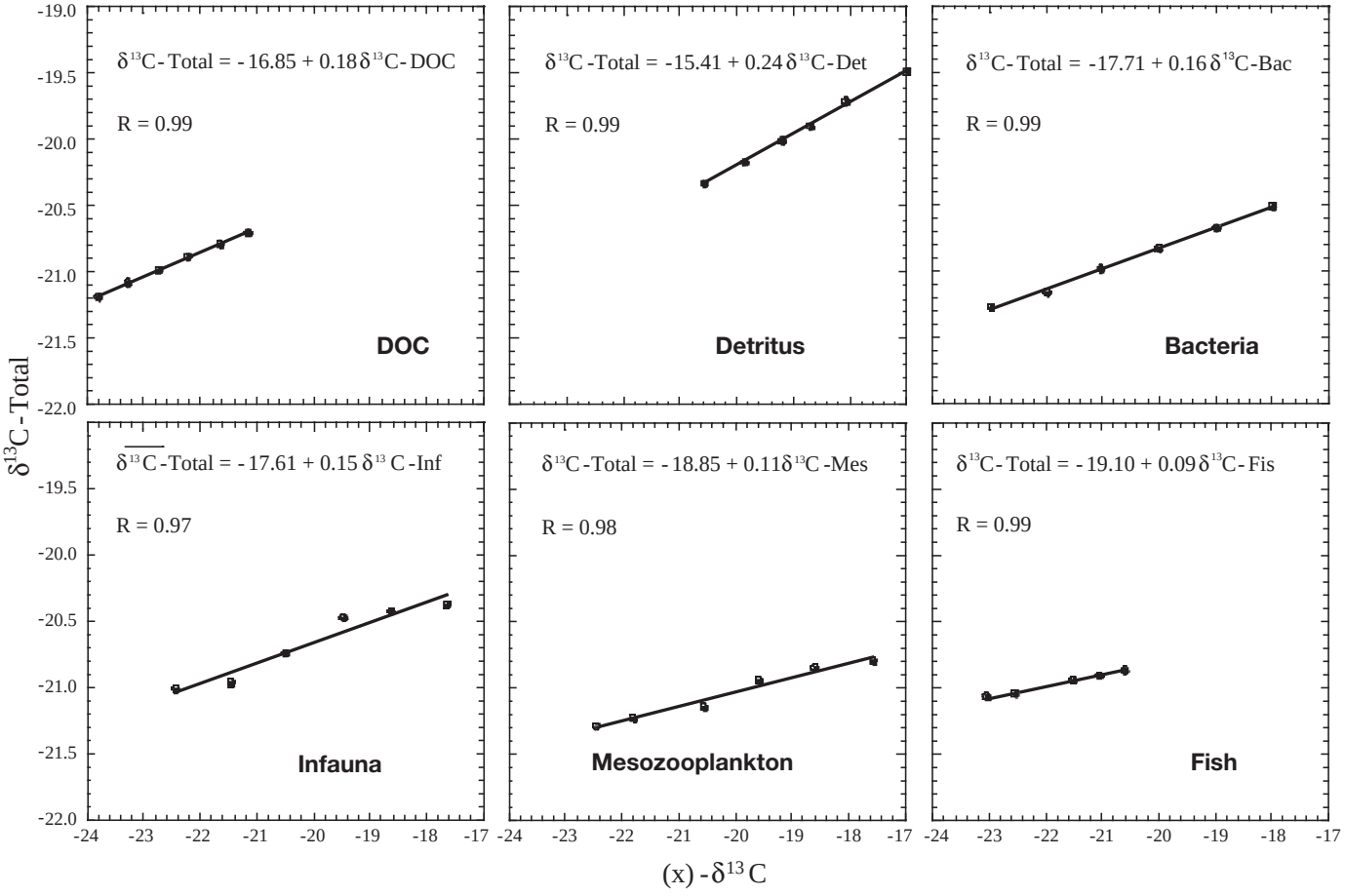

Fig. 4. Variation among model runs with different $\delta^{13}C$ stable-isotope inputs, showing how $\delta^{13}C$ individual food web components affects integrated food-web. Regressions show relationship between weighted $\delta^{13}C$ of flows for DOC, detritus, bacteria, infauna, mesozooplankton, and fishes and the weighted (by flow size) $\delta^{13}C$(total food web)

tope ratio had a larger effect on the sensitivity parameters than did changes in the flux data. The values of *S*(*Cm*,*p*) for the stable isotopes were largest for the infauna, and were in sequentially decreasing values for Rincon Delta, river input and phytoplankton; macroalgae; detritus. The trophic fractionation factors had a relatively modest effect on the simulations. The maximum effect of the isotope data was >100%, while that for the flux was about 40%. The *S*(*N-RMSD*,*p*) generally mirrored trends shown by the *S*(*Cm*,*p*) sensitivity parameter for changes in the stable isotope ratios but were often 1 order of magnitude lower than the *S*(*Cm*,*p*) (Table 6).

DISCUSSION

Role of stable-isotope constraints

The isotope constraints had no effect on the autotrophic components of the food web but dramatically affected the size of the heterotrophic food-web flows, rates of organic carbon burial and export to Corpus Christi Bay. Of the biotic components, the benthic infauna, mesozooplankton and fishes were most affected: both physiological losses and feeding rates were different when the isotope constraints were used in the model, but there was no obvious trend of increasing or decreasing rates. Without isotopic constraints, the models predicted that the sediment infauna metabolized considerably different amounts of carbon 23% more metabolism in the flood model and 12% less metabolism in the dry model than when isotopic constraints were used. Community respiration differed by 13% between the isotopically constrained and unconstrained dry model, but was about the same for the constrained and unconstrained flood models.

How the isotopic constraints enhanced model accuracy is difficult to evaluate. However, with the isotopic equations and inequalities in place, the optimization estimated more flows with values that did not coincide with a constraint boundary (often called a sticky or active constraint when the boundary determines the

Table 6. Parameter sensitivity. Model was run at parameter values p ± 0.2 of a standard case (high inundation). Carbon (grazer:community) respiration-sensitivity parameters, *S*(*Cm*,*p*) show normalized responses to changes in data *p* + (1.2 of normal value); and *p* – (0.8 of normal parameter value). If *S* = 100%, 20% change in data would lead to 20% change in result (see 'Materials and methods — sensitivity to model parameters' for details). Similarly, generalized fit parameter *S*(*N-RMSD*,*p*) was calculated for each model parameter. As with *S*(*Cm*), 20% change in a parameter that alters result by 20% will have a *S*(*N-RMSD*,*p*) of 1. Herbivore (1‰) and carnivore (2‰) trophic fractionations were changed simultaneously. ns: no solution

Model parameter (*p*)	Values		*S*(*Cm*,*p*)		*S*(*N-RMSD*,*p*)	
	min.	max.	min.	max.	min.	max.
Stable-isotope data ($\delta^{13}C$)						
Atmosphere	–8.0	–	2.2	–5.3	–1.8	1.9
DIC, river	–2.0	–	4.0	–4.0	–1.8	1.7
DIC, coastal	–1.9	–	4.0	–4.0	–1.8	1.8
Phytoplankton	–21.9	–	40.9	124.2	–22.8	15.3
Macroalgae	–16.8	–	ns	117.7	ns	11.5
DOC	–23.7	–	4.0	ns	–1.8	ns
Mesozooplankton	–18.30	–	–72.5	ns	–10.4	ns
Infauna	–20.5	–	ns	–227.2	ns	16.3
Fishes	–18.80	–	–14.3	ns	–3.3	ns
Detritus	–22.7	–19.3	–107.9	ns	–10.4	ns
River	–29.0	–27.0	71.7	124.0	–13.0	10.8
Delta	–27.0	–23.0	–18.4	124.0	–18.5	10.8
Sediment	–19.0	–	2.4	1.9	–2.4	3.4
Trophic fractionation	1 & 2	–	13.2	12.6	–1.3	1.3
Flux data (mmol C m^{-2} d^{-1})						
DOC from river	3.1	–	5.6	–6.3	–1.3	0.8
Detritus from river	7.3	58.3	5.6	–5.6	–1.2	1.2
Detritus from delta	37.0	116.7	–1.5	–10.4	–3.8	3.0
DOC from delta	40.0	146.7	–2.5	–9.5	–5.6	5.6
Phytoplankton	25.0	56.3	43.1	40.5	–4.5	4.5
Benthic algae	2.4	8.4	4.0	–4.0	–1.8	1.8
Mesozooplankton	2.1	3.18	4.0	–4.0	–1.8	1.8
Infauna	4.2	9.8	4.0	–4.0	–1.8	1.8
Sediment DIC	21.0	107.0	–33.3	–41.4	–4.2	3.9
Burial	4.2	9.8	5.6	–5.6	–1.2	1.2

value of a flow). When a constraint is not active, the information content of the flows concerned is higher, since presumably more constraint information is involved in the prediction of the flow. In the dry simulation, the flows predicted by the model suggested a relative equivalence of infauna and mesozooplankton in Nueces Bay, even though the bounds for consumption and respiration were quite different (Table 1). A relative equivalency between mesozooplankton and infauna consumption rates might not be expected in other shallow Texas estuaries, where higher benthic infauna abundances are found (Montagna & Kalke 1992, 1995, Montagna & Li 1996), but is probably reasonable for Nueces Bay, where infauna abundance is low but mesozooplankton abundance is similar to that in other South Texas estuaries (Buskey 1989, Montagna & Kalke 1992, Longley 1994).

The ability of the isotopically constrained model to add complexity to the food-web analysis is a major step forward in inverse-modeling. As pointed out by Vezina & Platt (1988) and Jackson & Eldridge (1992), the minimization technique generally used in these analyses provides the simplest pathway for material flows in a network. Our sensitivity tests showed that the stable isotopes provide additional information that the model can use to predict interspecies interactions generally missing from previous inverse analyses.

The sensitivity tests suggest that the isotope ratio of individual populations can be used to predict the integrated $\delta^{13}C$ of the food web. Given the large difference in the $\delta^{13}C$ of allochthonous and autochthonous sources to Nueces Bay, we might infer the impact these sources have on the estuarine food web simply by measuring $\delta^{13}C$ of a few components of the food web. Detritus was the best predictor of the $\delta^{13}C$(total), but $\delta^{13}C$ measurements of this pool would suffer from re-suspension of sediments due to tidal and wind wave turbulence. DOC, bacteria and infauna were also good predictors of the systems state. However, because infauna have life cycles similar to the residence time of the estuary, their isotope ratio would probably be the best estimator of the systems state over temporal periods close to the residence time of Nueces Bay.

Effect of freshwater marsh inundation

As pointed out earlier ('Results — Models'), the data for the dry and flood analyses were the same except for changes in freshwater input rates and $\delta^{13}C$ of Rincon Delta detritus and DOC, so the details of these analyses cannot be expected to truly characterize these events. However, our analysis showed some attributes that were consistent with our knowledge of the effect of freshwater inflows and inundation. Our simulations showed that infaunal production increased with freshwater inundations. Similarly, Montagna & Kalke (1992) showed that benthic macrofauna production was stimulated by freshwater inflow pulses. This was not true for meiofauna communities, but macrofauna data was used in the model. That the model seemed to follow known patterns of infaunal production relative to freshwater inflow further suggests infauna as a good bio-indicator of Nueces Bay food-web processes.

Carbon flux through the DOC compartment was about the same for the flood and dry simulations. Only 35 to 40% of the carbon flux through the DOC compartment was used by bacteria and about 50% of this utilizable DOC had been previously processed by heterotrophs. Network analysis showed that nearly all the DOC released by the autotrophs was used directly by bacteria, as opposed to only 20% DOC from the river and delta. The DOC and detritus from the Delta are probably considerably more refractory to bacterial and other heterotrophic consumption than are the autochthonous DOC or detritus (Benner et al 1991, Heip et al. 1995). In both model scenarios (flood and dry models), bacterial production was less than 25% of primary production. Benner & Yoon (1989) reported bacterial production between 1 and 30% of primary production in Nueces Bay, with an average of 10%. Our analyses suggest that, even with the relatively long water-retention time scale in Nueces Bay, most DOC released from Rincon Delta or the river is eventually exported from Nueces Bay.

In contrast to the DOC dynamics, there was 63% more exchange of carbon through the detritus compartment in the flood than in the dry model, but except for the infauna this did not result in additional heterotrophic production. Instead, most of the detrital carbon was exported from Nueces Bay. The input–output analysis using NETWRK suggests that in both simulations about 45% of the allochthonous carbon from the Rincon Delta marsh and the river moved through Nueces Bay with no interactions with the food web.

While fresh detrital material from marsh grass is reactive, older (>10 mo) detrital material has been shown to be relatively unreactive on the timescales of Nueces Bay hydraulic residence-time (Benner et al. 1991). Even if this material should be deposited in Nueces Bay sediments, its metabolism is slow relative to autochthonous sources of depositional carbon (Heip et al. 1995), and it may contribute more to the buried pool of organic carbon and less to the pool of more reactive carbon that re-enters the estuary as DIC.

Equality and inequality relationships

The inverse model with stable-isotope constraints provides a quantitative set of results that are generally consistent with our understanding of isotope geochemistry. The model is robust against small changes in data, yet sensitive to large changes in single food-web compartments (Fig. 4). There are, however, model attributes that need to be considered when applying isotope constraints. Although small differences in the isotope ratio of physiological flows from a single organism might be expected, they are generally related to isotope fractionation (Hatch et al 2002, Ayliffe et al 2004). Equality relationships are the only mechanism in our inverse model formulation to provide a consistent set of isotopical outflows from a single model compartment. Inequalities were used for the upper and lower bounds of non-living compartments since they have no associated physiological flows. We were able to produce an inverse analysis using only stable isotope equality relationships, but found that many of the flows in our standard model became zero. The combination of linear equations for biological compartments and linear inequalities for non-living compartments produced food-web solutions with the most non-zero flows.

Finally $\delta^{13}C$ signatures can be highly variable in time and space even within a functional group such as phytoplankton, macrozooplankton, infauna and sediments (Gearing et al 1984, Goering et al 1990); hence there is always a concern that data collected at different times will not be comparable. Most of the biotic stable-isotope data in this analysis were from a single study of Nueces Bay (Parker et al 1989); however much of the data for non-living compartments was collected at a later date (see Table 2). Isotope data for biotic components were formulated as equations requiring a more synoptic data set. The non-living compartments were formulated as a set of inequalities that bound ranges of isotope data. Hence the model can select the most appropriate value from the inequalities based on other input data. To characterize estuarine-scale food webs, investigators will to some extent have to rely on historical data; however, ideally stable-isotope data should be collected as nearly synoptically as possible.

Acknowledgements. Financial support for this work was provided by grants from Texas Parks and Wildlife Department and Texas Water Development Board. Field support was provided by personnel from Texas Parks and Wildlife and C. Carneal from Texas A&M University. We thank Donald Phillips, Scott Larned and 2 anonymous reviewers for their suggestions. Mention of trade names or commercial products does not constitute endorsement or recommendation for use.

LITERATURE CITED

Alexander H, Dunton KH (2002) Freshwater inundation effects on emergent vegetation of a hypersaline salt marsh. Estuaries 25:1426–1435

Ayliffe LK, Cerling TE, Robinson T, West AG and 6 others (2004) Turnover of carbon isotopes in tail hair and breath CO_2 of horses fed an isotopically varied diet. Oecologia 139:11–22

Benner R, Yoon W (1989) Nitrogen cycling and bacterial production: final report to Texas Water Development Board. University of Texas at Austin, Marine Science Institute, Marine Laboratory, Port Aransas, TX

Benner R, Fogel ML, Sprague EK (1991) Diagensis of belowground biomass of *Spartina alterniflora* in salt-marsh sediments. Limnol Oceanogr 36:1358–1374

Bianchi TS, Baskaran M, DeLord J, Ravichandran M (1997) Carbon cycling in a shallow turbid estuary of southeast

Texas: the use of plant pigment biomarkers and water quality parameters. Estuaries 20:404–415
Bricker SB, Ferreira JG, Simas T (2003) An integrated methodology for assessment of estuarine trophic status. Ecol Model 169:39–60
Brock DA (2001) Nitrogen budget for low and high freshwater inflows, Nueces Estuary, Texas. Estuaries 24:509–521
Bureau of Reclamation (2000) Concluding report: Rincon Bayou Demonstration Project, Vol I: Executive Summary; Vol II.: Findings. US Department of Interior, Bureau of Reclamation, Oklahoma–Texas Area Office, Austin, TX
Buskey EJ (1989) Effects of freshwater inflow on the zooplankton of Texas coastal bays. Report to Texas Water Development Board. Marine Science Institute, University of Texas at Austin, Port Aransas, TX
Cloern J (2001) Our evolving conceptual model of the coastal eutrophication problem. Mar Ecol Prog Ser 210:223–253
Coffin RB, Cifuentes LA, Eldridge PM (1994) The use of stable carbon isotopes to study microbial processes in estuaries. In: Kemp PF, Sherr BF, Sherr EB, Cole JJ (eds) Current methods in aquatic microbial ecology. Lewis Publishers, Boca Raton, FL, p 222–240
Craig H (1953) Carbon-13 in plants and the relationships between carbon-13 and carbon-14 variations in nature. J Geol 62:115–149
Dunton KH, Hardegree B, Whitledge TE (2001) Response of estuarine marsh vegetation to interannual variations in precipitation. Estuaries 24:851–861
Eldridge PM, Jackson GA (1993) Benthic trophic dynamics in California coastal basin and continental slope communities inferred using inverse analysis. Mar Ecol Prog Ser 99: 115–135
Fasham MJR, Ducklow HW, McKelvie SM (1990) A nitrogen-based model of plankton dynamics in the oceanic mixed layer. J Mar Res 48:591–639
Fogel ML, Cifuentes LA (1993) Isotopic fractionation during primary production. In: Engel M, Macko SA (eds) Organic geochemistry. Plenum Press, New York, p 73–98
Gearing JN, Gearing PJ, Rudnick DT, Requejo AG, Hutchins MT (1984) Isotopic variability of organic carbon in a phytoplankton-based, temperate estuary. Geochim Cosmochim Acta 48:1089–1098
Goering J, Alexander V, Haubenstock N (1990) Seasonal variability of stable carbon and nitrogen ratios of organisms in a North Pacific Bay. Estuar Coast Shelf Sci 30:239–260
Hatch KA, Pinshow B, Speakman JR (2002) The analysis of $^{13}C/^{12}C$ ratios in exhaled CO_2: its advantages and potential application to field research to infer diet, changes in diet over time, and substrate metabolism in birds. Integr Comp Biol 42:21–33
Heip CHR, Goosen NK, Herman PM, Kromkamp JJ, Middleburg JJ, Soetart K (1995) Production and consumption of biological particles in temperate tidal estuaries. Oceanogr Mar Biol Annu Rev 33:1–149
Hopkinson CS, Vallino JJ (1995) The relationship among man's activities in watersheds and estuaries: a model of runoff effects on patterns of estuarine community metabolism. Estuaries 18:598–621
Jackson GA, Eldridge PM (1992) Foodweb analysis of a planktonic system off southern California. Progr Oceanogr 30:223–251
Kaldy JE, Onuf CP, Eldridge PM, Cifuentes LA (2002) Carbon budget for a sub-tropical seagrass dominated coastal lagoon: how important are seagrasses to total ecosystem primary production? Estuaries 25:528–539
Lajtha K, Michener RH (eds) (1994) Stable isotopes in ecology and environmental science. Blackwell Scientific, Oxford
Longley WL (ed) (1994) Freshwater inflows to Texas bays and estuaries: ecological relationships and methods for determination of needs. Texas Water Development Board and Texas Parks and Wildlife Department, Austin, TX p 1–386
Mantoura RFC, Llewellyn CA (1983) The rapid determination of algal chlorophyll and caratenoid pigments and their breakdown products in natural waters by reversed-phase high-performance liquid chromatography. Anal Chim Acta 151:297–314
McCutchan JH, Lewis WM, Kendall C, McGraph CC (2003) Variation in trophic shift for stable isotope ratios of carbon, nitrogen, and sulfur. Oikos 102:378–390
Minagawa M, Wada E (1984) Stepwise enrichment of ^{15}N along food chains: further evidence and relationship between $\delta^{15}N$ and animal age. Geochim Cosmochim Acta 48:1135–1140
Montagna PA, Kalke RD (1992) The effect of freshwater inflow on meiofaunal and macrofaunal populations in the Guadalupe and Nueces Estuaries, Texas. Estuaries 15: 307–326
Montagna PA, Kalke RD (1995) Ecology of infaunal mollusca in south Texas estuaries. Am Malacol Bull 11:163–175
Montagna PA, Li J (1996) Modeling and monitoring long-term changes in macrobenthos in Texas estuaries. University of Texas, Marine Science Institute, UTMSI Tech Rep TR/96–001, p 150
Niquil, N, Jackson GA, Lengendre L, Delesalle B (1998) Inverse model analysis of the plankton food web of Takapoto Atoll (French Polynesia). Mar Ecol Prog Ser 165:17–29
Nixon S, Granger SL, Nowicki BL (1996) The fate of nitrogen and phosphorus at the land–sea margin of the North Atlantic Ocean. Biogeochemistry 35:141–180
Nixon S, Buckley B, Granger SL, Bintz J (2001) Responses of very shallow marine ecosystems to nutrient enrichment. Hum Ecol Risk Assess 7:1457–1481
Parker PL, Dunton KH, Scalan RS, Anderson RK (1989) Final integrated report, stable isotope component: report to Texas Water Development Board. Marine Science Institute, University of Texas at Austin, Port Aransas, TX
Parsons TR, Takahashi M, Hargrave B (1984) Biological oceanographic processes, 3rd edn. Pergamon Press, New York
Penniman CA, Mathieson AC (1987) Variation in chemical composition of *Gracilaria tikvahiae* McLahlan (Girtinales, Rhodophyta) in the Great Bay Estuary, New Hampshire. Bot Mar 30:525–534
Peterson BJ, Fry B (1987) Stable isotopes in ecosystem studies. Annu Rev Ecol Syst 18:293–320
Post DM (2002) Using stable isotopes to estimate trophic position: models, methods, and assumptions. Ecology 83: 703–718
Pulich WM, Scalan RS (1987) Organic carbon and nitrogen flow from marine cyanobacteria to semi aquatic insect food chains. Contrib Mar Sci 30:27–37
Roelke DL (1997) Managing phytoplankton community composition. Can we do it? PhD thesis, Texas A&M University, College Station, TX
Roelke DL, Eldridge PM, Cifuentes LA (1999) A model of phytoplankton competition for limiting and non-limiting nutrients: implications for development of estuarine and nearshore management schemes. Estuaries 22:92–104
Salata GG, LA Roelke, LA Cifuentes (1996) A rapid and precise method for the determination of dissolved inorganic carbon stable isotopes. In: Spargo BJ (ed) *In situ* bioremediation and efficacy monitoring. NRL/PU/6115–96–317. Naval Research Laboratory, Washington DC, p 79–85
Stockwell DA (1989) Effects of freshwater inflow on the primary production of a Texas coastal bay system. Board

Report to the Water Development. Marine Science Institute, University of Texas at Austin, Port Aransas, TX
Twilley RR, Cowan J, Miller-Way T, Montagua PA, Mortazvi B (1999) Benthic nutrient fluxes in selected estuaries in the Gulf of Mexico. In: Bianchi TS, Pennoch JR, Twilley RR (eds) Biogeochemistry of Gulf of Mexico estuaries. John Wiley & Sons, New York, p 162–210
Ulanowicz RE, Kay JJ (1986) NETWRK3: a package of computer algorithims to analyze ecological flow networks. UMCEES Ref No. 82–7C CBL. University of Maryland, Solomons, MD
Vezina AF, Platt T (1988) Food web dynamics in the ocean: best-estimates of flow networks using the inverse methods. Mar Ecol Prog Ser 42:269–287
Vezina AF, Savenkoff C, Roy S, Klein B, Rivkin R, Therriault JC, Legendre L (2000) Export of biogenic carbon and structure and dynamics of the pelagic food web in the Gulf of St. Lawrence. Part 2. Inverse analysis. Deep-Sea Res II 47:609–635
Vezina AF, Berreville F, Loza S (2004) Inverse reconstructions of ecosystem flows in investigating regime shifts: impact of the choice of objective function. Prog Oceanogr 60:321–341
Vollenweider RA (1975) Input–output models with special reference to the phosphorus loading concept in limnology. Schweiz Z Hydrol 37:53–84
Volterra V (1926) Variazioni e fluttuazioni del numero d'individui in specie animali conviventi. Mem R Acad Naz dei Lincei Ser VI 2:31–113
Wahlen M (1994) Carbon dioxide, carbon monoxide and methane in the atmosphere: abundance and isotopic composition. In: Lajtha K, Michener RH (eds) Stable isotopes in ecology and environmental science. Blackwell Scientific, Oxford, p 93–113
Ward GH, Irlbeck MJ, Montagna PA (2002) Experimental river diversion for marsh enhancement. Estuaries 25: 1416–1425
Weilhoefer CL (1998) Effects of freshwater inflow, salinity and nutrients on marsh vegetation in South Texas. Masters thesis, University of Texas at Austin, Port Aransas, TX

Appendix 1. Model formulation, showing equations and constraints used in Nueces estuary model. Formulation is same for both the 'flood' and 'dry' models (see Tables 1 & 2 for input data used in equations and constraints for models). Abbreviations for model compartments, flux and biomass data as in Tables 1 & 4A. *T* in biomass-dependent expressions: temperature (°C); C: carbon flow ('flow' in Eqs. 1 to 5 replaced by C for brevity); first subscript: source compartment, second subscript: destination compartment; α_1 and α_2: isotope trophic fractionations equivalent to 1 or 2 $^{13}\Delta$C. α_3: isotopic fractionation for primary production, equivalent to –20 $^{13}\Delta$C

Compartment	Equations describing mass balance
C-phytoplankton	$C_{dic,phy} - C_{phy,dic} - C_{phy,det} - C_{phy,doc} - C_{phy,mes} - C_{phy,inf} - C_{phy,fis} = 0$
C-benthic algae	$C_{dic,mal} - C_{mal,dic} - C_{mal,det} - C_{mal,doc} - C_{mal,mes} - C_{mal,inf} - C_{mal,fis} = 0$
C-bacteria	$C_{doc,bac} - C_{bac,dic} - C_{bac,doc} - C_{bac,det} - C_{bac,mes} - C_{bac,inf} = 0$
C-mesozooplankton	$C_{phy,mes} + C_{mal,mes} + C_{bac,mes} + C_{det,mes} - C_{mes,dic} - C_{mes,doc} - C_{mes,det} - C_{mes,fis} - C_{mes,exp} = 0$
C-infauna	$C_{phy,inf} + C_{mal,inf} + C_{bac,inf} + C_{det,inf} - C_{inf,dic} - C_{inf,sed} - C_{inf,doc} - C_{inf,fis} = 0$
C-fish	$C_{phy,fis} + C_{mal,fis} + C_{det,inf} + C_{mes,fis} + C_{inf,fis} + C_{riv,fis} + C_{del,fis} - C_{fis,dic} - C_{fis,det} - C_{fis,doc} - C_{fis,exp} = 0$
C-detritus	$C_{phy,det} + C_{mal,det} + C_{bac,det} + C_{mes,det} + C_{fis,det} - C_{det,mes} + C_{riv,det} + C_{del,det} - C_{det,inf} - C_{det,fis} - C_{det,doc} - C_{det,sed} = 0$
C-sediment	$C_{inf,sed} + C_{riv,sed} + C_{det,sed} + C_{det,sed} - C_{sed,dic} - C_{sed,bur} = 0$
C-dissolved organic carbon	$C_{phy,doc} + C_{mal,doc} + C_{mes,doc} + C_{inf,doc} + C_{fis,doc} + C_{bac,doc} + C_{det,doc} + C_{riv,doc} + C_{del,doc} - C_{doc,bac} - C_{doc,exp} = 0$
C-dissolved inorganic carbon	$C_{phy,dic} + C_{mal,dic} + C_{bac,dic} + C_{mes,dic} + C_{inf,dic} + C_{fis,dic} + C_{sed,dic} + C_{atm,dic} - C_{dic,phy} - C_{dic,mal} - C_{dic,atm} - C_{dic,exp} = 0$
Definition	**Isotope equalities**
CO_{2aq} to atmosphere	$-r_{co2aq}\,{}^{12}C_{dic,atm} + {}^{13}C_{dic,atm} = 0$
Atmosphere to CO_{2aq}	$-r_{co2at}\,{}^{12}C_{atm,dic} + {}^{13}C_{atm,dic} = 0$
Corpus Chisti Bay to DIC	$-r_{dic,exp}\,{}^{12}C_{dic,exp} + {}^{13}C_{dic,exp} = 0$
DIC to Corpus Chisti Bay	$-r_{exp,dic}\,{}^{12}C_{exp,dic} + {}^{13}C_{exp,dic} = 0$
Phytoplankton production	$-r_{dic,phy}\alpha_3\,{}^{12}C_{dic,phy} + {}^{13}C_{dic,phy} = 0$
Phytoplankton respiration	$-r_{phy}\,{}^{12}C_{phy,dic} + {}^{13}C_{phy,dic} = 0$
phy-mes consumption	$-r_{phy}\,{}^{12}C_{phy,mes} + {}^{13}C_{phy,mes} = 0$
phy-inf consumption	$-r_{phy}\,{}^{12}C_{phy,inf} + {}^{13}C_{phy,inf} = 0$
phy-fis consumption	$-r_{phy}\,{}^{12}C_{phy,fis} + {}^{13}C_{phy,fis} = 0$
phy-det death	$-r_{phy}\,{}^{12}C_{phy,det} + {}^{13}C_{phy,det} = 0$
phy-doc excretion	$-r_{phy}\,{}^{12}C_{phy,doc} + {}^{13}C_{phy,doc} = 0$
Macroalgae production	$-r_{dic,mal}\,\alpha_3\,{}^{12}C_{dic,\,mal} + {}^{13}C_{dic,\,mal} = 0$
Macroalgae respiration	$-r_{mal}\,\alpha_1\,{}^{12}C_{mal,dic} + {}^{13}C_{,mal,dic} = 0$
mal-mes consumption	$-r_{mal}\,{}^{12}C_{mal,mes} + {}^{13}C_{mal,mes} = 0$
mal-inf consumption	$-r_{mal}\,{}^{12}C_{mal,inf} + {}^{13}C_{mal,inf} = 0$

Appendix 1 (continued)

mal-fis consumption	$-r_{mal}\ {}^{12}C_{mal,fis} + {}^{13}C_{mal,fis} = 0$
mal-det death	$-r_{mal}\ {}^{12}C_{mal,det} + {}^{13}C_{mal,det} = 0$
mal-doc excretion	$-r_{mal}\ {}^{12}C_{mal,doc} + {}^{13}C_{mal,doc} = 0$
mes-dic respiration	$-r_{mes}\ a_1\ {}^{12}C_{mes,dic} + {}^{13}C_{mes,dic} = 0$
mes-det fecal/death	$-r_{mes}\ {}^{12}C_{mes,det} + {}^{13}C_{mes,det} = 0$
mes-doc excretion	$-r_{mes}\ {}^{12}C_{mes,doc} + {}^{13}C_{mes,doc} = 0$
mes-fis consumption	$-r_{mes}\ {}^{12}C_{mes,fis} + {}^{13}C_{mes,fis} = 0$
inf-dic respiration	$-r_{inf}\ a_1\ {}^{12}C_{inf,dic} + {}^{13}C_{inf,dic} = 0$
inf-sed fecal/death	$-r_{inf}\ {}^{12}C_{inf,sed} + {}^{13}C_{inf,sed} = 0$
inf-doc excretion	$-r_{inf}\ {}^{12}C_{inf,doc} + {}^{13}C_{inf,doc} = 0$
inf-fis consumption	$-r_{inf}\ {}^{12}C_{inf,fis} + {}^{13}C_{inf,fis} = 0$
fis-dic respiration	$-r_{fis}\ a_2\ {}^{12}C_{fis,dic} + {}^{13}C_{fis,dic} = 0$
fis-det fecal/death	$-r_{fis}\ {}^{12}C_{fis,det} + {}^{13}C_{fis,det} = 0$
fis-doc excretion	$-r_{fis}\ {}^{12}C_{fis,doc} + {}^{13}C_{fis,doc} = 0$
fis-exp consumption	$-r_{fis}\ {}^{12}C_{fis,exp} + {}^{13}C_{fis,exp} = 0$
bac-dic respiration	$-r_{bac}\ {}^{12}C_{bac,dic} + {}^{13}C_{bac,dic} = 0$
bac-mes consumption	$-r_{bac}\ {}^{12}C_{bac,mes} + {}^{13}C_{bac,mes} = 0$
bac-inf consumption	$-r_{bac}\ {}^{12}C_{bac,inf} + {}^{13}C_{bac,inf} = 0$
bac-det death	$-r_{bac}\ {}^{12}C_{bac,det} + {}^{13}C_{bac,det} = 0$
bac-doc excretion	$-r_{bac}\ {}^{12}C_{bac,det} + {}^{13}C_{bac,det} = 0$
sed-dic respiration	$-r_{sed}\ {}^{12}C_{sed,dic} + {}^{13}C_{sed,dic} = 0$

Definition		Inequalities
Phytoplankton net primary production	min	$C_{dic,phy} - C_{phy,dic} - C_{doc,phy} \geq NPP_{phy\_lo}$
	max	$-C_{dic,phy} + C_{phy,dic} + C_{doc,phy} \geq -NPP_{phy\_hi}$
Benthic algae net primary production	min	$C_{dic,phy} - C_{phy,dic} - C_{doc,phy} \geq NPP_{mal\_lo}$
	max	$-C_{dic,phy} + C_{phy,dic} + C_{doc,phy} \geq -NPP_{mal\_hi}$
Bacterial production	min	$C_{doc,bac} \geq P_{bac}$
River DOC	min	$C_{riv,doc} \geq FDOC_{riv}$
River sediment	min	$C_{riv,sed} \geq Fsed_{riv\_lo}$
	max	$-C_{riv,sed} \geq -Fsed_{riv\_hi}$
Delta export	min	$C_{del,doc} + C_{del,det} \geq FOC_{del\_lo}$
	max	$-C_{del,doc} - C_{del,det} \geq -FOC_{del\_hi}$
Burial	min	$C_{sed,bur} \geq Fbur_{est\_lo}$
	max	$-C_{sed,bur} \geq -Fsed_{est\_hi}$
Mesozooplankton production	min	$C_{phy,mes} + C_{mal,mes} + C_{bac,mes} + C_{det,mes} \geq GP_{mes\_lo}$
Infaunal production	min	$C_{phy,inf} + C_{mal,inf} + C_{bac,inf} + C_{det,inf} \geq GP_{inf\_lo}$
Phytoplankton respiration	min	$C_{phy,dic} - 0.05C_{dic,phy} \geq 0$
	max	$-C_{phy,dic} + 0.3C_{dic,phy} \geq 0$
Phytoplankton excretion	min	$C_{phy,doc} - 0.05C_{dic,phy} \geq 0$
	max	$-C_{phy,doc} + 0.5C_{dic,phy} \geq 0$
Benthic algae respiration	min	$C_{mal,dic} - 0.05C_{dic,mal} \geq 0$
	max	$-C_{mal,dic} + 0.3C_{dic,mal} \geq 0$
Benthic algae excretion	min	$C_{mal,doc} - 0.05C_{dic,mal} \geq 0$
	max	$-C_{mal,doc} + 0.5C_{dic,mal} \geq 0$
Mesozooplankton respiration	min	$C_{mes,dic} \geq B_{meslo}\ e^{0.0693\ T}$
Mesozooplankton excretion	min	$C_{mes,doc} - 0.33C_{mes,dic} \geq 0$
	max	$-C_{mes,doc} + C_{mes,dic} \geq 0$
Mesozooplankton assimilation eff.	min	$-0.5\ (C_{phy,mes} + C_{mal,mes} + C_{bac,mes} + C_{det,mes}) + C_{mes,doc} \geq 0$
	max	$-0.1\ (C_{phy,mes} + C_{mal,mes} + C_{bac,mes} + C_{det,mes}) + C_{mes,doc} \geq 0$

Appendix 1 (continued)

Infauna excretion	min	$C_{inf,doc} - 0.33C_{inf,dic} \geq 0$
	max	$-C_{inf,doc} + C_{inf,dic} \geq 0$
Fish excretion	min	$C_{fis,doc} - 0.33C_{fis,dic} \geq 0$
	max	$-C_{fis,doc} + C_{fis,dic} \geq 0$
Bacteria assimilation	min	$0.9C_{doc,bac} - C_{bac,dic} - C_{bac,doc} \geq 0$
	max	$-0.4C_{doc,bac} + C_{bac,dic} + C_{bac,doc} \geq 0$
Infaunal assimulation efficiency	min	$0.5(C_{phy,inf} + C_{mal,inf} + C_{bac,inf} + C_{det,inf}) \geq C_{inf,doc}$
	max	$-0.1(C_{phy,inf} + C_{mal,inf} + C_{bac,inf} + C_{det,inf}) \geq -C_{inf,doc}$
Infaunal respiration	min	$C_{inf,dic} \geq 0.006\ B_{inf\_lo}e^{0.0693\ T}$
Fish consumption	min	$C_{phy,fis} + C_{mal,fis} + C_{mes,fis} + C_{mes,fis} + C_{det,fis} \geq 0.1\ B_{fis}e^{0.0693\ T}$
Fish assimilation efficiency	min	$0.5\ (C_{phy,fis} + C_{mal,fis} + C_{mes,fis} + C_{mes,fis} + C_{det,fis} \geq C_{fis,doc}$
	max	$-0.1\ (C_{phy,fis} + C_{mal,fis} + C_{mes,fis} + C_{mes,fis} + C_{det,fis}\ ) \geq C_{fis,doc}$
Fish respiration	min	$C_{fis,dic} \geq 0.005\ B_{fis\_lo}e^{0.0693\ T}$
Mesozooplankton gross-production efficiency	min	$0.9\ (C_{phy,mes} + C_{mal,mes} + C_{bac,mes} + C_{det,mes}) - C_{mes,det} - C_{mes,doc} - C_{mes,dic} - C_{mes,fis} \geq 0$
	max	$-0.1\ (C_{phy,mes} + C_{mal,mes} + C_{bac,mes} + C_{det,mes}) + C_{mes,det} + C_{mes,doc} + C_{mes,dic} + C_{mes,fis} \geq 0$
Infauna gross-production efficiency	min	$0.9\ (C_{phy,inf} + C_{mal,inf} + C_{bac,inf} + C_{det,inf}) - C_{inf,det} - C_{inf,doc} - C_{inf,dic} - C_{inf,fis} \geq 0$
	max	$-0.1\ (C_{phy,inf} + C_{mal,inf} + C_{bac,inf} + C_{det,inf}) + C_{inf,det} + C_{inf,doc} + C_{inf,dic} \geq 0$
Fish gross-production efficiency	min	$0.9\ (C_{phy,fis} + C_{mal,fis} + C_{bac,fis} + C_{det,fis}) - C_{fis,det} - C_{fis,doc} - C_{fis,dic} \geq 0$
	max	$-0.1\ (C_{phy,fis} + C_{mal,fis} + C_{bac,fis} + C_{det,fis}) + C_{fis,det} + C_{fis,doc} + C_{fis,dic} \geq 0$
Definition		**Isotope inequalities**
det-mes consumption	min	$-r_{det\_lo}\ {}^{12}C_{det,mes} + {}^{13}C_{det,mes} \geq 0$
	max	$r_{det\_hi}\ {}^{12}C_{det,mes} - {}^{13}C_{det,mes} \geq 0$
det-inf consumption	min	$-r_{det\_lo}\ {}^{12}C_{det,inf} + {}^{13}C_{det,inf} \geq 0$
	max	$r_{det\_hi}\ {}^{12}C_{det,inf} - {}^{13}C_{det,inf} \geq 0$
det-fis consumption	min	$-r_{det\_lo}\ {}^{12}C_{det,fis} + {}^{13}C_{det,fis} \geq 0$
	max	$r_{det\_hi}\ {}^{12}C_{det,fis} - {}^{13}C_{det,fis} \geq 0$
det-doc consumption	min	$-r_{det\_lo}\ {}^{12}C_{det,doc} + {}^{13}C_{det,doc} \geq 0$
	max	$r_{det\_hi}\ {}^{12}C_{det,doc} - {}^{13}C_{det,doc} \geq 0$
det-sed	min	$-r_{det\_lo}\ {}^{12}C_{det,sed} + {}^{13}C_{det,sed} \geq 0$
	max	$r_{det\_hi}\ {}^{12}C_{det,sed} - {}^{13}C_{det,sed} \geq 0$
doc-phy consumption	min	$-r_{doc\_lo}\ {}^{12}C_{doc,phy} + {}^{13}C_{doc,phy} \geq 0$
	max	$r_{doc\_hi}\ {}^{12}C_{doc,phy} - {}^{13}C_{doc,phy} \geq 0$
doc-bac consumption	min	$-r_{doc\_lo}\ {}^{12}C_{doc,bac} + {}^{13}C_{doc,bac} \geq 0$
	max	$r_{doc\_hi}\ {}^{12}C_{doc,bac} - {}^{13}C_{doc,bac} \geq 0$
riv-doc transport	min	$-r_{riv\_lo}\ {}^{12}C_{riv,doc} + {}^{13}C_{riv,doc} \geq 0$
	max	$r_{riv\_hi}\ {}^{12}C_{riv,doc} - {}^{13}C_{riv,doc} \geq 0$
riv-det transport	min	$-r_{riv\_lo}\ {}^{12}C_{riv,det} + {}^{13}C_{riv,det} \geq 0$
	max	$r_{riv\_hi}\ {}^{12}C_{riv,det} - {}^{13}C_{riv,det} \geq 0$
riv-fis transport	min	$-r_{riv\_lo}\ {}^{12}C_{riv,fis} + {}^{13}C_{riv,\ fis} \geq 0$
	max	$r_{riv\_hi}\ {}^{12}C_{riv,fis} - {}^{13}C_{riv,fis} \geq 0$
del-doc transport	min	$-r_{del\_lo}\ {}^{12}C_{del,doc} + {}^{13}C_{del,doc} \geq 0$
	max	$r_{del\_hi}\ {}^{12}C_{del,doc} - {}^{13}C_{del,doc} \geq 0$
del-det transport	min	$-r_{del\_lo}\ {}^{12}C_{del,det} + {}^{13}C_{del,det} \geq 0$
	max	$r_{del\_hi}\ {}^{12}C_{del,det} - {}^{13}C_{del,det} \geq 0$
del-fis transport	min	$-r_{del\_lo}\ {}^{12}C_{del,fis} + {}^{13}C_{del,fis} \geq 0$
	max	$r_{del\_hi}\ {}^{12}C_{del,fis} - {}^{13}C_{del,fis} \geq 0$
det-exp transport	min	$-r_{det\_lo}\ {}^{12}C_{det,exp} + {}^{13}C_{det,exp} \geq 0$
	max	$r_{det\_hi}\ {}^{12}C_{det,exp} - {}^{13}C_{det,exp} \geq 0$
doc-exp transport	min	$-r_{doc\_lo}\ {}^{12}C_{doc,exp} + {}^{13}C_{doc,exp} \geq 0$
	max	$r_{doc\_hi}\ {}^{12}C_{doc,exp} - {}^{13}C_{doc,exp} \geq 0$

Editorial responsibility: Otto Kinne (Editor-in-Chief), Oldendorf/Luhe, Germany

Submitted: September 24, 2003; Accepted: May 19, 2005
Proofs received from author(s): October 31, 2005